

Magnetic field driving custom assembly in (FeCo) nanocrystals

P. Marín, M. López, A. Vlad, A. Hernando, M. L. Ruiz-González, and J. M. González-Calbet

Citation: *Applied Physics Letters* **89**, 033508 (2006); doi: 10.1063/1.2222254

View online: <http://dx.doi.org/10.1063/1.2222254>

View Table of Contents: <http://scitation.aip.org/content/aip/journal/apl/89/3?ver=pdfcov>

Published by the [AIP Publishing](#)

Articles you may be interested in

Investigation on high-temperature magnetic permeability of Si-rich nanocrystalline (Fe_{0.9}Co_{0.1})_{74.5}Nb₂Si_{17.5}B₅Cu₁ alloy

J. Appl. Phys. **117**, 17B701 (2015); 10.1063/1.4906297

Crystallization behavior and high temperature magnetic phase transitions of Nb-substituted FeCoSiBCu nanocomposites

Appl. Phys. Lett. **99**, 192506 (2011); 10.1063/1.3660245

Influence of magnetic field annealing on saturation magnetostriction and μ -T curves for FeCo-based nanocrystalline alloy

J. Appl. Phys. **109**, 07A328 (2011); 10.1063/1.3562969

Enhanced magnetic properties of FeCo ribbons nanocrystallized in magnetic field

Appl. Phys. Lett. **94**, 122507 (2009); 10.1063/1.3091401

Recent advances in the development of (Fe_{0.8}Co_{0.2})₈₈M₇B₄Cu₁ magnets (invited)

J. Appl. Phys. **87**, 7091 (2000); 10.1063/1.372941

SHARE


your expertise in
simulation


TE11 cutoff frequency (fc):	4.868 Hz
Frequency:	fc*1.2 Hz
Wavelength (λ):	0.5205 m
Flare angle:	17 °
Corrugation thickness:	0.105 m
Corrugation length:	0.155 m
Horn thickness:	0.5 m
Horn length:	4 m
Waveguide length:	1 m
Matching corrugation length:	0.25 m

WITH COMSOL APPS »

Input waveguide cross pol. ratio:	17.657 %
Output aperture cross pol. ratio:	3.025 %

Target criterion: passed





Magnetic field driving custom assembly in (FeCo) nanocrystals

P. Marín,^{a)} M. López, A. Vlad, and A. Hernando

*Departamento de Física de Materiales, Instituto de Magnetismo Aplicado,
Universidad Complutense de Madrid, P.O. Box 155, Las Rozas, 28230 Madrid, Spain*

M. L. Ruiz-González and J. M. González-Calbet

*Departamento de Química Inorgánica, Universidad Complutense de Madrid, Avenida Complutense s/n,
28040 Madrid, Spain*

(Received 10 March 2006; accepted 11 June 2006; published online 21 July 2006)

We present the possibility of tuning the nanocrystalline microstructure of Co-rich samples by magnetic field annealing. Custom assembly of nucleated grains, aligned in the field direction, has been observed by means of high resolution transmission microscopy. The organized microstructure was obtained on the basis of the appropriate choice of composition, annealing temperature, related to the initial stages of nanocrystallization process, and magnetic field intensity. The linear pattern of the grains has been explained as a consequence of the counterbalance between magnetic, magnetostatic, and magnetocrystalline couplings, only relevant when the nucleation temperature is well below the Curie temperature of the nucleated phase. © 2006 American Institute of Physics. [DOI: 10.1063/1.2222254]

The first nanocrystalline alloys presenting soft magnetic behavior were iron based.¹ Other compositions were also studied. The last series concerns FeCo based alloys^{2,3} technologically promising at high temperature. Nanocrystalline iron based samples are obtained by partial crystallization of amorphous alloys.⁴ Its nanocrystalline microstructure is constituted by bcc Fe-Si with grain sizes of 10–15 nm with a fractional volume of 75%, from which their soft properties derive. Softness mainly arises from the averaging out of magnetocrystalline anisotropy via the magnetic interactions between the two constituent magnetic phases reinforced by a decrease of magnetoelastic energy.⁴ The control of amorphous percentage and grain size should be done through composition and annealing temperature^{5,6} of the initial amorphous alloy. Other studies have been focused in the possibility of inducing magnetic anisotropy by means of annealing nanocrystalline materials in the presence of magnetic field.⁴

In this letter, we present the possibility of tuning the structure of Co-rich nanograins by means of magnetic field annealing. In contrast with results reported for Fe-rich alloys, we have observed a noticeable influence of magnetic field on nanocrystallization of $\text{Fe}_{28.5}\text{Co}_{45}\text{Si}_{13.5}\text{B}_9\text{Cu}_1\text{Nb}_3$ (FeCo-rich alloys) that present Curie temperature and spontaneous magnetization higher than those of Fe-rich alloys.⁶ We provide strong evidence that applied field during the first stage of nanocrystallization, at 733 K, exerts a drastic influence on both percentage of crystallized material and size of the precipitated fcc FeCoSi (Ref. 7) grains. Moreover, the effect of the applied field is also reflected in the assembly of nanograins that show aligned patterns as well as crystalline texture with an order degree that increases with the intensity of the applied field. The field induced directional order is characterized by a decrease of the intergrain distance along the field direction when compared to the perpendicular one. The possibility of tuning directional order by using a magnetic field opens interesting perspectives concerning the rapid growth of controlled nanostructures.

Amorphous ribbons of composition $\text{Fe}_{28.5}\text{Co}_{45}\text{Si}_{13.5}\text{B}_9\text{Cu}_1\text{Nb}_3$ were obtained by melt-spinning technique of dimensions $0.5\text{ mm} \times 20\text{ }\mu\text{m} \times 60\text{ mm}$ were 1 h annealed, between 573 and 823 K, in argon atmosphere under magnetic fields, parallel to ribbon longitudinal direction, between 800 and 11 200 A m⁻¹. Crystallization dynamics and amorphous percentage have been obtained by means of calorimetric measurements, of as-cast and annealed samples, and were carried out in a differential scanning calorimeter (Perkin-Elmer DSC 7) operating at a fixed scanning rate. The x-ray diffractograms were obtained by using the copper $\lambda=0.1541\text{ nm}$ line (Siemens D5000). The microstructural study has been performed by means of transmission electron microscopy (JEOL JEM 3000 FX) and x-ray energy dispersive spectroscopy (XEDS). The hysteresis loops were obtained by conventional 80 Hz induction technique, while saturation magnetization of the samples was determined by vibrating sample magnetometer (VSM). Magnetization thermal dependence was made by means of effective magnetic weight in a thermobalance (CANH D-200) using a small permanent magnet giving 1600 A/m, field enough to saturate the sample.

The thermal evolution of the alloy from its initial state is shown in the calorimetric curve of Fig. 1(a). Two exothermic peaks, at 724 and 806.8 K, respectively, define three different stages I, II, and III, as shown in Fig. 1(a). For samples annealed between 553 and 713 K (stage I) the x-ray diffractogram shows the characteristic halo of amorphous systems, whereas a set of crystalline peak characteristic of a fcc cell, Fe_3Si type, appears for both stages II and III. According to x-ray reflections the partially devitrified state corresponding to stage II is mainly composed of ferromagnetic $\text{Fe}_{50-60}\text{Co}_{25-30}\text{Si}_{15-20}$ crystals as indicated by the XEDS analysis. The presence of Co, difficult to estimate from diffractograms, is clearly pointed out by the high value of the Curie temperature, 1123 K, when compared to those obtained by nanocrystallization of Fe-rich amorphous alloys, 923 K.⁶ According to the maximum observed at $2.8293\text{ }\text{\AA}$ that corresponds to (2,2,0) reflection, the Co content of the

^{a)}Electronic mail: pmarin@renfe.es

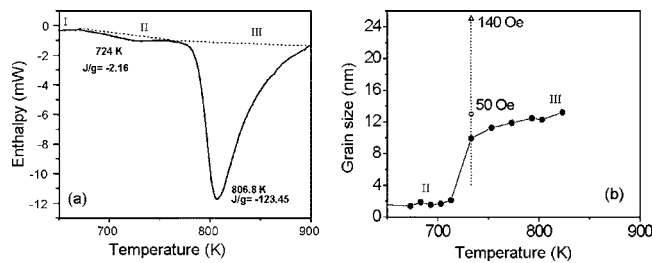


FIG. 1. (a) Differential scanning calorimetry of an as prepared $\text{Fe}_{28.5}\text{Co}_{45}\text{Si}_{13.5}\text{Cu}_1\text{Nb}_3$ sample at a scan rate of 20 K min^{-1} . The areas enclosed by each peak, in units of energy release per gram of sample, are shown in the figure. The two exothermic peaks separate stages I, II, and III, discussed in the text. (b) Grain size evolution with annealing temperature obtained from x-ray diffraction. The observed influence of magnetic field on crystal size at 733 K annealing temperature has been included.

crystallites increases up to a nominal composition $\text{Fe}_{34}\text{Co}_{50}\text{Si}_{16}$ (Ref. 6) at stage III. From the linewidth of the diffraction reflections, the average size of the crystallites has been estimated and its evolution with annealing temperature is shown in Fig. 1(b). The crystallized volume fraction was estimated by DSC analysis.

Figure 2 shows electron micrographs of the alloy annealed at 733 K for 1 h under 0, 4000, and 11 200 A m^{-1} magnetic fields. For the sample annealed without field a random distribution of grains of around 6 nm surrounded by an amorphous matrix is observed [Fig. 2(a)], confirming the x-ray diffraction data and calorimetric measurements that indicate a crystallized volume fraction of 10%. However, for the sample annealed in the presence of 4000 A m^{-1} magnetic field (volume fraction 24%) a grain assembly characterized by directional order, along the field direction, is observed [Fig. 2(b)]. A linear pattern governs the grain growth. This effect is associated with an increase of grain size to 10 nm and grain junction, as observed in Fig. 2(b).

The effect at 11 200 A m^{-1} is shown in Fig. 2(c), a co-existence of nanocrystalline aligned grains with amorphous matrix is still present. An increase of crystal size to 25 nm is coherent with the increase of crystallized fraction up to 40%. Moreover, the linear grain assembly increases. The high resolution electron microscopy (HREM) study of these samples confirms the fcc structure of the crystalline particles. As a representative example a HREM image and its corresponding fast Fourier transform (FFT) of a particle of the sample annealed without magnetic field are depicted in Fig. 2(d). The observed influence of magnetic field on crystal size

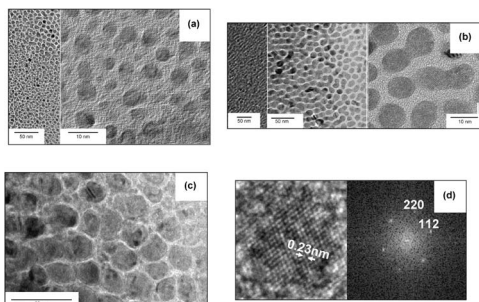


FIG. 2. Micrographs of the $\text{Co}_{45}\text{Fe}_{28.5}\text{Si}_{13.5}\text{B}_9\text{Cu}_1\text{Nb}_3$ alloy annealed at 733 K for 1 h under 0 (a), 4000 (b), and 11 200 A m^{-1} (c) magnetic fields. As a representative example a HREM image and its corresponding fast Fourier transform (FFT) of a particle of the sample annealed without magnetic field are depicted (d).

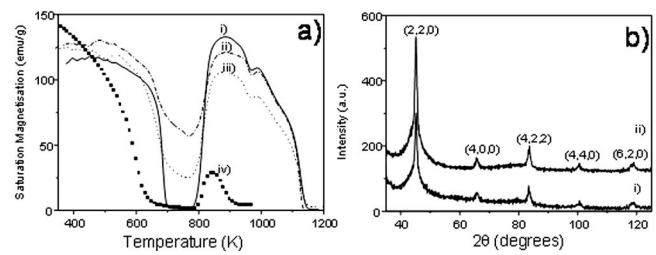


FIG. 3. (a) Magnetization under a constant field dc vs the measuring temperature for $\text{Co}_{45}\text{Fe}_{28.5}\text{Si}_{13.5}\text{B}_9\text{Cu}_1\text{Nb}_3$: as-cast sample (i) and annealed at 733 K at 0 (ii) and 11 200 A m^{-1} (iii) and $\text{Fe}_{73.5}\text{Si}_{13.5}\text{B}_9\text{Cu}_1\text{Nb}_3$: as-cast sample (iv). (b) X-ray diffraction patterns for annealed $\text{Co}_{45}\text{Fe}_{28.5}\text{Si}_{13.5}\text{B}_9\text{Cu}_1\text{Nb}_3$ samples at 733 K without magnetic field (i) and in the presence of 4000 A m^{-1} (ii) magnetic field.

at 733 K annealing temperature has been included in Fig. 1(b).

The magnetic/microstructural description of samples was completed by measuring magnetization under a constant field dc versus the measuring temperature for as-cast sample and annealed at 733 K at 0 and 11 200 A m^{-1} , as shown in Fig. 3. The magnetization evolution with temperature for the sample without cobalt, with composition $\text{Fe}_{73.5}\text{Si}_{13.5}\text{B}_9\text{Cu}_1\text{Nb}_3$, has also been included. In both cases, for the amorphous sample the magnetization $\sigma(T)$ decreases down to zero at the amorphous Curie temperature. Further heating induces a sharp $\sigma(T)$ increase, towards higher magnetization values in the case of cobalt based sample than in the free one, related to the onset of crystallization process. In the case of annealed samples, due to previous partial crystallization, the samples remain ferromagnetic at and above the amorphous Curie temperature. However, the corresponding decrease of magnetization exhibited by the field annealing sample is much smaller than that corresponding to the zero field annealing sample. This difference is also due to the difference in crystalline fraction for both samples.

Figure 4(a) shows a HREM micrograph for 733 K annealed sample at 4000 A m^{-1} . An enhanced image of a particle and its corresponding FT along $[1\bar{1}0]$ [Fig. 4(b)] show the lattice distances and the $[110]$ direction is arrowed, confirming the preferential direction shown by x-ray diffraction (XRD) in Fig. 3(b). It is important to remark that fcc Fe-Co-Si magnetocrystalline anisotropy is characterized by easy axes along the $[110]$ direction.

Previous works show the subsequent microstructure of annealed samples.⁹ It has been suggested that the applied field can act as a driving force for directional grain nucleation through the magnetic free energy. Magnetocrystalline

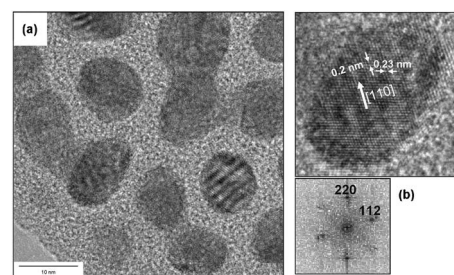


FIG. 4. HREM micrograph for 733 K annealed $\text{Co}_{45}\text{Fe}_{28.5}\text{Si}_{13.5}\text{B}_9\text{Cu}_1\text{Nb}_3$ sample at 4000 A m^{-1} (a). An enhanced image of a particle and its corresponding FT along $[1\bar{1}0]$ (b) show the lattice distances and the $[110]$ direction is arrowed.

anisotropy and magnetostriction gradients between different phases have been invoked to account for texture generation during crystallization process.⁹

Let us analyze the possible origin of the experimental results reported here. If we define the polar orientation as that of the magnetic field, Fig. 2(b) indicates that when a grain is nucleated in a particular reference point the probability of a subsequent nucleation at the neighborhood increases at the polar orientation with respect to the equatorial one. The probability of nucleation is governed by the nucleation free energy e . Such energy, even though extended over an energy spectrum and dependent on the distance to the previously nucleated grain, is randomly distributed in orientation as confirmed by the crystallite pattern observed in the sample annealed in the absence of applied field, Fig. 2(a). With the effect of the applied field the spherical symmetry is broken. The anisotropic nucleation probability can be described by introducing in the activation energy of the neighborhood e a bias term that at first order can be written as $-e_H(3 \cos^2 \theta - 1)$, where θ is the polar angle of the line joining the previously nucleated grain and the new nucleated grain. It is obvious that magnetostatic interactions account for this tendency with an approximated e_H given by $\mu_0 M_z^2 (v_1 v_2 / 4 \pi r^3)$, where v_1 and v_2 are, respectively, the volumes of the interacting grains and r is the distance between their centers. Note that M_z , the average magnetization of the nucleated phase along the field direction at the annealing temperature, must rise with the applied field H to reach its saturation value. Most of the nucleated grains should behave as superparamagnetic at 733 K. Consequently, the increase of H from 4000 up to 11 200 A m⁻¹ should induce an increase of e_H through the increase in M_z , as reflected in the experimental results. As H increases further, M_z approaches its saturation value M_s , and e_H reaches its higher value $\mu_0 M_s^2 (v_1 v_2 / 4 \pi r^3)$. For constant grain size and applied field, e_H exhibits thermal dependence through both the thermal dependence of the superparamagnetic susceptibility and that of $M_s(T)$. As a general condition it should be considered that e_H is an increasing function of $(T_c - T)$, T_c being the Curie temperature of the grains nucleated at T .

Nucleation is observed at temperatures T for which $e \sim k_B T$, k_B being the Boltzmann constant. The processes activated during annealing at 733 K are those with energy close to 10⁻²⁰ J. The bias effect of the field should also be noticeable only if $e_H(T)$ is close to $k_B T$. From the pattern shown in Fig. 2(a), that provides $v_1 = v_2 = 10^{-25}$ m³, $r = 10^{-8}$ m, estimation of e_H yields, $e_H = \mu_0 M_s^2 10^{-27}$ J. As an effect of the Co content, the Curie temperature of crystallites is enhanced up to 1123 K much above than the annealing temperature of 733 K; consequently, the spontaneous magnetization of the crystallites at 733 K is high enough to contribute decisively to e_H . In the case of FeCo-Si grains $\mu_0 M_s$ is close to 1.5 T at room temperature and remains above 1 T at 733 K.⁶ Therefore, e_H that is then about 10⁻²¹ J equivalent to 70 K,—i.e., close to e —can induce observable directional order. However, Fe-rich crystallites⁶ as shown in Fig. 3, with Curie temperature of 923 K, nucleate at 823 K, temperature at which the spontaneous magnetization is below 0.3 T. For this last case e_H falls down one order of magnitude below e and its

effect on the kinetics and subsequent microstructure becomes negligible.

When the applied field is high enough to produce complete magnetization alignment, the activation energy for nucleation decreases to $e - 2e_H$ along the polar axis. Therefore, the effective annealing temperature for polar nucleation and growth is 870 K, whereas for transverse crystallization decreases down to 660 K. Consequently, the nucleation and growth rate at 733 K are expected to be that obtained without applied field at an intermediate effective temperature, i.e., 800 K. This effect explains the experimentally observed tendency to increase polar growth rate and consequently connectivity between grains and crystallized volume fraction. In particular, the 40% crystallized fraction obtained after annealing at 733 K under a field of 11 200 A m⁻¹ [Fig. 2(c)] has also been reached after annealing at 790 K in the absence of field. The field effect experimentally obtained is then equivalent to a 57 K effective increase of the annealing temperature, in good agreement with our previous estimation. Finally, the [110] texture can be associated with the magnetocrystalline anisotropy energy. As magnetostatic energy tends to align grain(s) along the magnetization direction and the magnetization is required by both applied field and easy axes, the grain as a whole tends to align the easy axes along the polar or field direction. These arguments also account for the dependence of grain size, grain alignment, and crystalline texture on the intensity of the applied field as stated above.

In summary, we have shown that nanocrystalline grains can be directionally ordered by annealing of Fe_{28.5}Co₄₅Si_{13.5}Cu₁Nb₃ ribbons in the presence of magnetic field. This happens when the annealing temperature corresponds to the first stages of nanocrystallization process (stage II). The field effect can be described by a relative increase of the crystallized volume fraction and a linear alignment of the nucleated grains. The energy barrier for nucleation is directionally affected by the applied field. The effect only can merge when in the temperature range at which nucleation takes place, M_s is high enough to increase sufficiently these three free energy terms. This last condition holds if the Curie temperature of the nucleated phase is high enough to lie well above the temperature at which nucleation proceeds, as is the case for FeCo-Si nanocrystals.

¹Y. Yoshizawa, S. Oguma, and K. Yamauchi, J. Appl. Phys. **64**, 6044 (1988).

²M. A. Willard, D. E. Laughlin, M. E. Mchenry, D. Thoma, K. Sickafus, J. O. Cross, and V. G. Harris, J. Appl. Phys. **84**, 6773 (1988).

³G. Herzer, in *Handbook of Magnetic Materials*, edited by K. H. J. Buschow (Elsevier Science BV, The Netherlands, 1997), Vol. 10, pp. 415–462.

⁴K. Hono, A. Inoue, and T. Sakurai, Appl. Phys. Lett. **58**, 2180 (1991); P. Marín, M. Vázquez, A. O. Olofinjana, and H. A. Davies, Nanostruct. Mater. **10**, 299 (1998).

⁵M. Vázquez, P. Marín, H. A. Davies, and A. O. Olofinjana, Appl. Phys. Lett. **64**, 3184 (1994).

⁶C. Gómez-Polo, P. Marín, L. Pascual, A. Hernando, and M. Vázquez, Phys. Rev. B **65**, 024433 (2001).

⁷V. Niculescu, J. D. Budnick, W. A. Hines, K. Raj, S. Pickart, and S. Skalski, Phys. Rev. B **19**, 452 (1979).

⁸N. O. Eriksson, L. Bergqvist, E. Holström, O. Lebacqz, S. Frota-Pessoa, B. Hjörvarson, and L. Nordström, J. Phys.: Condens. Matter **15**, S599 (2003).

⁹H. O. Martikainen and V. K. Lindroos, Scand. J. Metall. **10**, 3 (1991); N. Masahashi, M. Matsuo, and K. Watanabe, J. Mater. Res. **13**, 457 (1998).